

## Positron Decay of $\text{Cu}^{59}$ and $\text{Cu}^{61}$ and Energy Levels in $\text{Ni}^{59}$ and $\text{Ni}^{61}$

J. W. BUTLER AND C. R. GOSSETT

*Nucleonics Division, United States Naval Research Laboratory, Washington, D. C.*

(Received October 11, 1957)

The energies and relative intensities of the gamma rays following the positron decay of  $\text{Cu}^{59}$  have been determined. The energies are  $0.343 \pm 0.004$ ,  $0.463 \pm 0.010$ ,  $0.872 \pm 0.005$ ,  $1.305 \pm 0.005$ , and  $1.70 \pm 0.01$  Mev, with respective relative intensities of  $16 \pm 3$ ,  $15 \pm 5$ ,  $29 \pm 4$ ,  $36 \pm 4$ , and  $4 \pm 2\%$ . The half-life of  $\text{Cu}^{59}$  was measured to be  $81.5 \pm 0.5$  seconds. The energies of ground-state transition gamma rays following the positron decay of  $\text{Cu}^{61}$  were measured as  $0.070 \pm 0.002$ ,  $0.282 \pm 0.003$ ,  $0.659 \pm 0.003$ , and  $1.192 \pm 0.005$  Mev. The accumulated works of several authors are discussed and compared.

### I. INTRODUCTION

At least 17 papers<sup>1-17</sup> were published between 1950 and 1955 on the masses and low-lying energy levels of  $\text{Ni}^{59}$  and  $\text{Ni}^{61}$ . In spite of all the activity concerning these two nuclides, a number of serious discrepancies were noted when the  $\text{Ni}^{58}(p,\gamma)\text{Cu}^{59}$  and  $\text{Ni}^{60}(p,\gamma)\text{Cu}^{61}$  reactions were studied.<sup>18</sup> A survey of the published information concerning  $\text{Ni}^{61}$  and the closely associated nuclide  $\text{Ni}^{59}$  (since  $\text{Ni}^{59}$  is often produced in the same reaction as  $\text{Ni}^{61}$ ) revealed that the data of the various experimenters were not in good agreement and that no consistent set of energy levels or ground-state masses could be assigned from the then available evidence. Therefore, it was considered worthwhile to investigate these two nuclides by several different techniques. Accordingly, the  $\text{Ni}^{58}(p,\gamma)\text{Cu}^{59}$  and  $\text{Ni}^{60}(p,\gamma)\text{Cu}^{61}$  reactions were studied in great detail.<sup>19</sup> That work included resonances,  $Q$  values, cross sections, gamma-cascade schemes, branching ratios, angular distributions, and partial resonance widths. The reaction  $\text{Co}^{59}(p,n)\text{Ni}^{59}$  was studied by Butler, Dunning, and Bondelid,<sup>20</sup> who found several slow-neutron thresholds corresponding to the ground state and several excited states of  $\text{Ni}^{59}$ . The gamma rays following the positron

decay of  $\text{Cu}^{59}$  and  $\text{Cu}^{61}$ , and assignments of energy levels therefrom, were measured and are reported herein.

### II. EXPERIMENTAL PROCEDURE

#### Gamma Rays

Targets of the separated isotopes<sup>21</sup> (99.6%  $\text{Ni}^{58}$  containing 0.3%  $\text{Ni}^{60}$ , and 98.5%  $\text{Ni}^{60}$  containing 1.5%  $\text{Ni}^{58}$ ) were prepared by electroplating 5–10 mg/cm<sup>2</sup> of nickel onto a 0.002-in. silver foil. The targets were then bombarded by a beam of 1.9-Mev protons (about 7  $\mu\text{a}$  for  $\text{Ni}^{58}$  and about 3  $\mu\text{a}$  for  $\text{Ni}^{60}$ ) from the NRL Nucleonics Division 2-Mv Van de Graaff accelerator for a time greater than a half-life of the residual nuclide (the half-life of  $\text{Cu}^{59}$  is 81 seconds, and that for  $\text{Cu}^{61}$  is 3.3 hours). The target (by then a source) was placed face up onto the end of a 3-in.  $\times$  3-in. NaI(Tl) crystal as shown in Fig. 1. The spectrum of gamma rays emitted following the positron decay was then determined with conventional pulse-measuring equipment including a 20-channel differential pulse-height analyzer. The 20-channel analyzer was "gated" to accept pulses only when they were in coincidence with a pulse in the thin Pilot-B phosphor directly above the source. Since the 0.012-in. thickness of Pilot-B phosphor had a very low efficiency for gammas, but a relatively high efficiency for betas, most of the gate pulses were initiated by a positron from the source passing through the phosphor. This positron could then be expected to annihilate in the vicinity of the phosphor. Because of the conical Pb shield shown in Fig. 1, the gate pulses would seldom be accompanied by the entrance of annihilation radiation into the NaI crystal. This gate requirement made it possible to observe low-intensity nuclear gammas near and below the peak of the annihilation radiation. A further beneficial effect of this particular coincidence arrangement is the strong reduction of "add up" true coincidences between a nuclear gamma ray and the annihilation radiation from the positron. This is especially important in determining the relative intensities of the gamma rays in this experiment because most of these gammas differ from their neighbors by about 500 kev.

<sup>21</sup> Obtained from the Stable Isotopes Division, Oak Ridge National Laboratory.

- <sup>1</sup> Owen, Cook, and Owen, *Phys. Rev.* **78**, 686 (1950).
- <sup>2</sup> Sher, Halpern, and Stephens, *Phys. Rev.* **81**, 154 (1951).
- <sup>3</sup> J. A. Harvey, *Phys. Rev.* **81**, 353 (1951).
- <sup>4</sup> H. E. Gove, *Phys. Rev.* **81**, 364 (1951).
- <sup>5</sup> J. J. G. McCue and W. M. Preston, *Phys. Rev.* **84**, 384 (1951).
- <sup>6</sup> Smith, Haslam, and Taylor, *Phys. Rev.* **84**, 842 (1951).
- <sup>7</sup> Collins, Nier, and Johnson, *Phys. Rev.* **86**, 408 (1952).
- <sup>8</sup> P. H. Stelson and W. M. Preston, *Phys. Rev.* **86**, 807 (1952).
- <sup>9</sup> D. C. Hoesterey, Ph.D. thesis, Yale University, 1952 (unpublished); *Phys. Rev.* **87**, 216(A) (1952), verbal report; quoted in *Nuclear Science Abstracts* **6**, No. 24B, 19 and 50 (1952).
- <sup>10</sup> B. B. Kinsey and G. A. Bartholomew, *Phys. Rev.* **89**, 375 (1953).
- <sup>11</sup> McFarland, Bretscher, and Shull, *Phys. Rev.* **89**, 892 (1953).
- <sup>12</sup> W. W. Pratt, *Phys. Rev.* **94**, 1086 (1954).
- <sup>13</sup> W. W. Pratt, *Phys. Rev.* **95**, 1517 (1954).
- <sup>14</sup> Nussbaum, Van Lieshout, Wapstra, Verster, Ten Haaf, Nijgh, and Ornstein, *Physica* **20**, 555 (1954).
- <sup>15</sup> Lindner, Brinkman, and Pieterse, *Physica* **21**, 745 (1955).
- <sup>16</sup> Yuasa, Nahmias, and Vivargent, *J. phys. radium* **16**, 654 (1955).
- <sup>17</sup> T. Yuasa and G. A. Renard, *J. phys. radium* **16**, 889 (1955).
- <sup>18</sup> Gossett, Butler, and Holmgren, *Bull. Am. Phys. Soc. Ser. II*, **1**, 40 (1956); **1**, 223 (1956).
- <sup>19</sup> J. W. Butler and C. R. Gossett, *Phys. Rev.* **108**, 1473 (1957).
- <sup>20</sup> Butler, Dunning, and Bondelid, *Phys. Rev.* **106**, 1224 (1957).

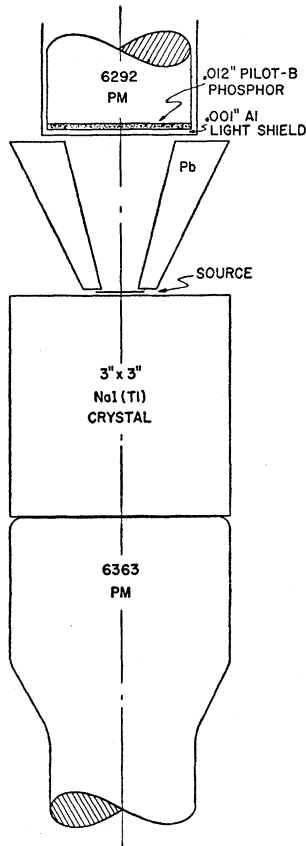


FIG. 1. Geometrical arrangement of gamma-ray spectrometer. Cylindrical symmetry was used.

To determine if any of the gamma rays were in cascade, the source was sandwiched between two 3-in.  $\times$  3-in. NaI crystals, placed end to end. The gains of the two systems were equalized, the anodes of the two phototubes were connected together, and the combined pulse was analyzed by the 20-channel analyzer. The analyzer was gated on by a coincidence between the No. 10 dynode pulses in each of the phototubes, with discrimination levels set at 450 kev. This requirement essentially eliminated the individual nuclear gamma peaks and materially reduced the sum peaks between one (or more) nuclear gamma ray and only one of the two annihilation quanta, because the probability of absorbing both annihilation quanta was greater than the probability of absorbing only one. This requirement did not affect the "grand sum" peak where both annihilation quanta added to the one (or more) nuclear gamma. Thus, from this arrangement, one would expect a 1.022-Mev peak where a positron left the residual nucleus in the ground state (and therefore no nuclear gammas in coincidence), or where the nuclear gamma was in the "equatorial plane" and therefore did not enter either crystal, or where one of the more penetrating nuclear gammas completely escaped the crystals. One would also expect a peak corresponding to each *energy level* of the residual nucleus added to 1.022 Mev. In addition there would be weaker peaks corresponding to

particular combinations of the nuclear gammas and annihilation quanta. Aluminum absorbers were placed on each side of the source to prevent the positrons themselves from entering the crystals.

To demonstrate the effect of this arrangement, Fig. 2 shows the  $\text{Na}^{22}$  decay spectrum under three different conditions. The dashed curve shows the spectrum when only one crystal is present, and therefore there is no coincidence requirement. The source is lying on the end of the crystal in the same location as it occupies when the other crystal is over it. Since the two annihilation quanta are emitted in opposite directions, there is no "grand sum" peak, because one or the other of the annihilation quanta is always lost. The solid curve shows the spectrum when both crystals are present, but with no coincidence requirement from the No. 10 dynodes of the phototubes. Note that we now have a 1.022-Mev peak corresponding to capture of both annihilation quanta; and we have a 2.299-Mev peak where both annihilation quanta and the nuclear gamma have been captured. The dot-dash curve shows the spectrum when the coincidence requirement is imposed that there be on each No. 10 dynode a pulse corresponding to at least 450 kev before a pulse can be analyzed and registered. Naturally, the curve goes to zero below 900 kev. The nuclear gamma peak disappears completely, and the sum peak between one annihilation quantum and the nuclear gamma is reduced by about a factor of two, but the grand sum peak is not affected.

### Half-Life

The half-life determination of  $\text{Cu}^{60}$  was made after bombarding the target for a period of about three half-lives (four minutes). The source was then placed face down onto the thin Pilot-B phosphor and the positrons counted for several half-lives. Precautions were taken to insure stability of gain and to maintain a uniform counting efficiency as a function of time.

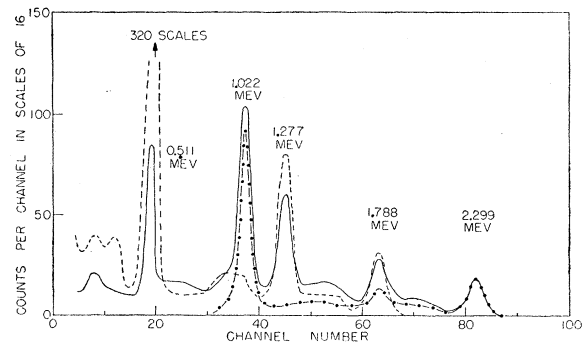


FIG. 2.  $\text{Na}^{22}$  decay spectrum. Dashed curve, one crystal. Solid curve, two crystals. Dot-dash curve, two crystals with coincidence requirement. The labeled peaks are (in order of increasing channel number): one annihilation quantum, two annihilation quanta, nuclear gamma ray, nuclear gamma ray plus one annihilation quantum, nuclear gamma ray plus two annihilation quanta.

Since electric clocks operating from the usual 60-cps power lines are frequently in error by about one percent when measuring short intervals, a 1000-cps driven tuning fork was used as the time standard in taking counts on the  $\text{Cu}^{59}$ . The 1000-cps vacuum-tube tuning fork was calibrated against the Naval Research Laboratory 100-kc standard. A scale-of-1000 was used to record precisely the end of each second.

### III. $\text{Cu}^{59}(\beta^+)\text{Ni}^{59}$

#### Gamma-Ray Spectrum

Figures 3 and 4 show the gamma-ray spectrum obtained with the arrangement in Fig. 1. The 75-kev peak is due to the x-ray from the Pb shield. It is caused by nuclear gamma rays or annihilation quanta ejecting  $K$  electrons from the Pb shield, and therefore the resulting x-ray sometimes occurs in true coincidence with a positron "gate" pulse from the Pilot-B phosphor. When the Pb shield was covered inside and out with a layer of 0.004-in. Sn and 0.005-in. Cu, the 75-kev peak, was not observed. The measured energy of the peak is based on a value of 82 kev for the  $\text{Ba}^{133}$  gamma ray. From tables of x-ray values, the energy should be about 73 kev. Note that the 463-kev nuclear gamma ray is not completely resolved from the 511-kev annihilation radiation. However, the resolution is good enough to reveal the presence of two peaks in this vicinity. Note also the width of the combined peak compared with that for the 343-kev gamma ray. In previous arrangements, the 511-kev radiation was so intense with respect to 463-kev gamma ray that the presence of the latter was not observable. In Fig. 4, the 1.816-Mev peak is caused by the adding up of a 1.305-Mev gamma ray and an annihilation quantum. There is no indication for a 2.06-Mev gamma ray reported by Prosser *et al.*<sup>22</sup> Perhaps our source was too weak for us to detect it. Neither is there

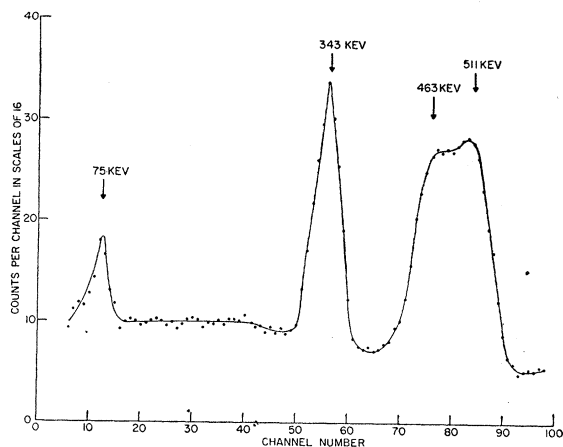


FIG. 3.  $\text{Cu}^{59}$  decay spectrum from 40 to 600 kev. The peak at 75 kev is due to the x-ray from the Pb cone.

<sup>22</sup> Prosser, Moore, and Schiffer, *Bull. Am. Phys. Soc. Ser. II*, **1**, 163 (1956).

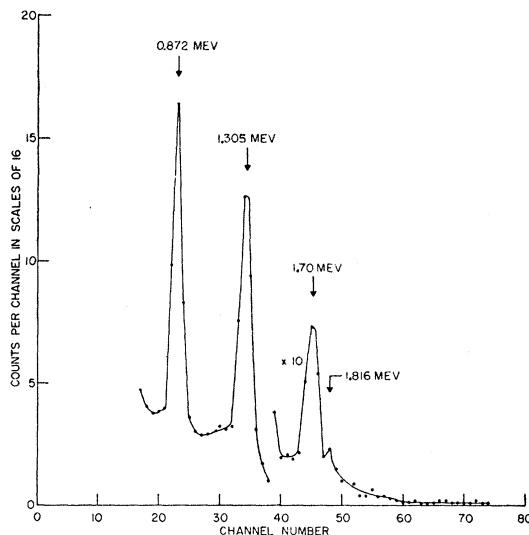


FIG. 4.  $\text{Cu}^{59}$  decay spectrum from 0.6 to 2.8 Mev. The 1.816-Mev peak represents the addition of an annihilation quantum to a 1.305-Mev quantum.

a peak of weak intensity corresponding to 190 kev as reported by us in a preliminary account<sup>23</sup> for which a different geometrical arrangement was used. It is believed that the previous weak indication for the 190-kev gamma ray was due to a small amount of backscattered Compton photons from the annihilation radiation, although precautions had been taken to avoid this effect.

#### Energy Measurements

The energies of the gamma rays were determined precisely by comparing the position of the spectrum peaks with known gamma-ray sources. The current in the phototube was made the same during calibrations as it was during the runs on the unknown gamma rays to insure gain stability. Calibrations were made before and after a run on the unknown. There were at least two calibration points for each gamma ray: one above and one below the unknown. This method of calibration made it possible to correct for nonlinearity in the amplifier or elsewhere in the system. The position of a peak was determined by taking several midpoints in the region of steepest rise and drawing a straight line through these points to intersect the curve in the region of the top. This point of intersection was considered the peak. Skewed peaks were automatically corrected for in this manner. Peaks could be determined repeatedly to within  $\frac{1}{10}$  of a channel by this procedure. This procedure is illustrated in Fig. 5, for the  $\text{Cu}^{61}$  decay, which is discussed in Sec. IV. For the combined 463- and 511-kev peak, the right and left sides were reflected about vertical lines whose positions were chosen to give

<sup>23</sup> Butler, Gossett, and Holmgren, *Bull. Am. Phys. Soc. Ser. II*, **1**, 163 (1956).

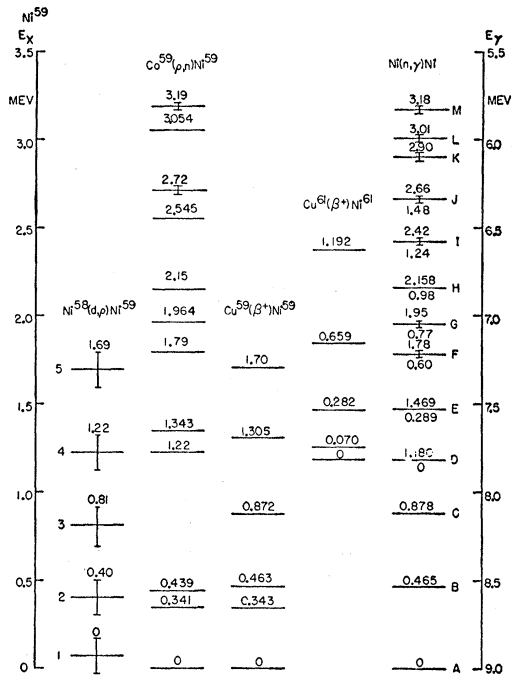


FIG. 5. A comparison of the energy levels of  $\text{Ni}^{59}$  and  $\text{Ni}^{61}$  as found by several different experiments. The columns from left to right present the data of references 13, 20, present, present, and 10, respectively. The energy scale on the right is that for neutron-capture gamma rays. The letters to the right of each level do not label the levels themselves, but represent the high-energy neutron-capture gamma ray, and were assigned to each individual gamma ray by Kinsey and Bartholomew. The numbers above each gamma-ray line give the energy state in  $\text{Ni}^{59}$ , assuming neutron capture by  $\text{Ni}^{58}$ . The numbers below each gamma-ray line give the energy state in  $\text{Ni}^{61}$ , assuming neutron capture by  $\text{Ni}^{60}$ .

the resulting component peaks the proper width. The area of overlap of the two peaks was then compared with the former area that was not included in either "constructed" peak. Ideally, these two areas should be equal, and they were equal within our limits of measurement. These vertical "reflection axes" were then considered to represent the center of the individual gamma peaks, and the energy of the unknown gamma was determined with respect to the 511-keV peak and  $\text{Ir}^{192}$  peak at 468 keV. A detailed examination of the combined peak with narrow channels (not illustrated) gave weak evidence of another gamma ray of about  $420 \pm 20$  keV. Such a gamma ray could be either a ground-state

TABLE I. Energies and relative intensities of gamma rays following the positron decay of  $\text{Cu}^{69}$ . Weak evidence was found for a gamma-ray energy of about  $0.42 \pm 0.02$  Mev and a relative intensity of about 5%.

Energy (Mev)	Based on	Relative intensity (%)
$0.343 \pm 0.004$	$0.316 \text{ Ir}^{192}$	$16 \pm 3$
$0.463 \pm 0.010$	$0.468 \text{ Ir}^{192}$	$15 \pm 5$
$0.872 \pm 0.005$	$0.662 \text{ Cs}^{137}$	$29 \pm 4$
$1.305 \pm 0.005$	$1.333 \text{ Co}^{60}$	$36 \pm 4$
$1.70 \pm 0.01$	$1.788 \text{ Na}^{22}$	$4 \pm 2$

transition from the 0.439-Mev state (see Sec. V) or a cascade from the 0.872-Mev state to either the 0.439-Mev state or the 0.465-Mev state. Table I gives the gamma-ray energies with probable errors and the primary calibrating standard used for each.

The 463-keV gamma ray has not previously been reported. The 343-keV gamma ray has been reported only in a preliminary account of the present experiment,<sup>23</sup> and the 1.70-Mev gamma ray has likewise been reported in abstract form.<sup>22,23</sup>

Figure 6 shows the double-crystal coincidence spectrum taken as described in Sec. II and illustrated by the dot-dash curve in Fig. 2 for the  $\text{Na}^{22}$  case. The 1.4-Mev peak corresponds to the addition of 1.022 Mev and the unresolved 0.34- and 0.46-Mev gamma rays, and the other peaks correspond to the addition of 1.022 Mev to each of the other gamma rays of Fig. 4,

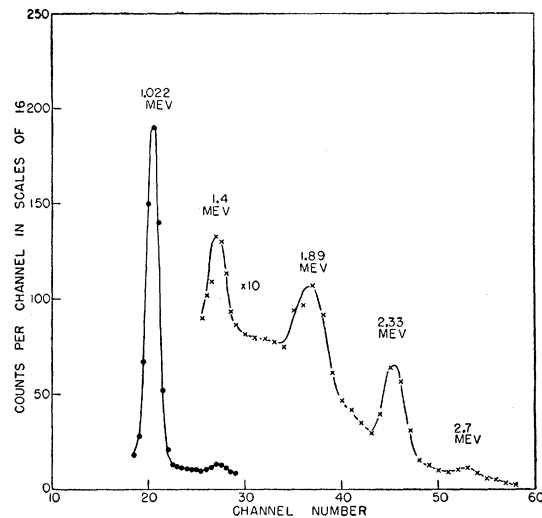


FIG. 6.  $\text{Cu}^{69}$  double-crystal coincidence spectrum. The lowest energy peak represents two annihilation quanta. The other peaks represent (in order of increasing channel number) two annihilation quanta plus: (1) the unresolved 0.343- and 0.463-Mev gamma rays, (2) the 0.872-Mev gamma ray, (3) the 1.30-Mev gamma ray, and (4) the 1.70-Mev gamma ray.

namely 0.87, 1.31, and 1.70 Mev. There is no peak corresponding to the addition of 1.022 Mev to the sum of any two nuclear gamma rays. Since the gammas are each independently in coincidence with the positrons but not with each other, it follows that they cannot be in cascade and cannot have lifetimes longer than our resolving time of  $0.2 \mu\text{sec}$ . Data taken without the coincidence requirement did not reveal any additional gamma rays.

### Relative Intensities

The relative intensity measurements were made by displaying two of the peaks simultaneously on the 20-channel analyzers. For these runs (which are not illustrated) the amplifier gain was adjusted to cause the

peaks in question to occupy at least five channels each. The relative intensities of the gamma rays were then obtained by taking the area under each photopeak, dividing it by a correction factor, and normalizing the sum to 100%. The correction factor included the intrinsic efficiency of the crystal as a function of gamma-ray energy, the attenuation of the gamma rays by the source backing and crystal covering, and the relative efficiency for the positron corresponding to a particular gamma ray to trigger the coincidence gate. The last correction was somewhat uncertain, but fortunately was small, the largest correction (for the 1.70-Mev gamma ray) amounting to less than 3% of the relative intensity. It was made by assuming an isotropic angular correlation between positron and gamma ray (which is believed to be valid for allowed transitions) and assuming a minimum energy of 150 keV to trigger the gate circuit (which would appear reasonable for a 0.001-in. Al window and 0.012-in. thick plastic phosphor). The contribution of the direct positrons was weighted, according to effective solid angle, with the back-scattered positrons from the silver backing, Al crystal cover,  $\text{MgO}_2$  reflector, NaI crystal, and the Pb collimator and shield. The decrease in energy of the back-scattered positrons was taken into account. The percentage of the effective positron spectrum below 150 keV was then calculated for each group of positrons (one group for each gamma) using the usual theoretical beta-spectrum functions, and this was used as a correction factor to determine relative gamma-ray intensities.

#### Half-Life

The half-life determination was made six times in the manner described in Sec. II, yielding values of 81.5, 81.4, 81.4, 81.4, 81.3, and 82.0 seconds. The average value is 81.5 seconds with an assigned uncertainty of  $\pm 0.5$  second. Each run covered at least nine half-lives.

Previous measurements of the half-life are (in seconds)  $81 \pm 2$ ,<sup>24</sup>  $81$ ,<sup>25</sup>  $82 \pm 1$ ,<sup>13</sup> and  $83 \pm 1$ .<sup>22</sup>

#### IV. $\text{Cu}^{61}(\beta^+)\text{Ni}^{61}$

Before the work on this reaction was finished, Nussbaum *et al.*<sup>26</sup> published a report on this same reaction. Since their work was in good agreement with our results to that point, our investigation of the  $\text{Cu}^{61}$  decay was not so complete as that of the  $\text{Cu}^{59}$  decay. We did not determine relative intensities or measure accurately the cascade energies or measure the half-life, since these are given by Nussbaum *et al.* We had already made careful energy measurements on the ground-state transitions, and present those in Table II. The measurement of the gamma-ray energies is illustrated in Fig. 7.

<sup>24</sup> Delsasso, Ridenour, Sherr, and White, Phys. Rev. **55**, 113 (1939).

<sup>25</sup> Leith, Bratenahl, and Moyer, Phys. Rev. **72**, 732 (1949).

<sup>26</sup> Nussbaum, Wapstra, Bruil, Sterk, Nijgh, and Grobden, Phys. Rev. **101**, 905 (1956).

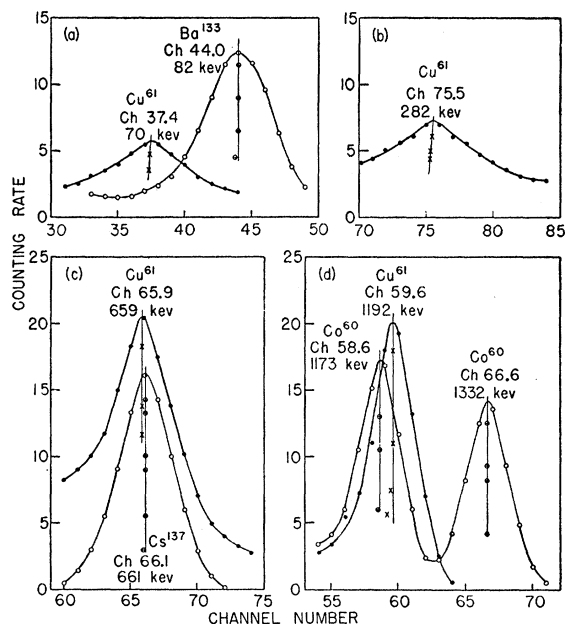


FIG. 7.  $\text{Cu}^{61}$  gamma-ray energy measurements. (a) 70-keV gamma ray with  $\text{Ba}^{133}$  calibration, (b) 282-keV gamma ray with calibration obtained by adjusting the gain of the pulse amplifier to be precisely half that used for (a), (c) 659-keV gamma ray with  $\text{Cs}^{137}$  calibration, (d) 1192-keV gamma ray with  $\text{Co}^{60}$  calibration.

#### V. DISCUSSION

As was promised in a previous communication,<sup>19</sup> an attempt will be made herein to accumulate the known evidence from this and other experiments and to assign a consistent set of energy levels to  $\text{Ni}^{59}$  and  $\text{Ni}^{61}$ . Kinsey and Bartholomew<sup>10</sup> measured rather precisely the high-energy gamma rays (5–9 MeV) resulting from thermal-neutron capture by natural nickel. Their isotopic assignments of the gamma rays were influenced by the mass-spectrometer determinations of the two mass doublets  $\text{C}_5\text{-Ni}^{60}$  and  $\text{C}_5\text{H-Ni}^{61}$  by Collins, Nier, and Johnson,<sup>7</sup> and by Hoestery's measurement<sup>9</sup> of the  $\text{Ni}^{60}(d,p)\text{Ni}^{61}$   $Q$  value. Using the mass-spectrometer values,<sup>7</sup> one calculates the  $\text{Ni}^{60}(d,p)\text{Ni}^{61}$  and  $\text{Ni}^{60}(n,\gamma)\text{Ni}^{61}$  reaction  $Q$  values to be  $6.1 \pm 0.3$  and  $8.3 \pm 0.3$  MeV, respectively. Hoestery's  $(d,p)$   $Q$  value<sup>9</sup> of  $6.30 \pm 0.04$  MeV is in good agreement with this particular set of mass-spectrometer data. On the basis of these data, Kinsey and Bartholomew assigned gamma-ray  $B$  (see Fig. 5) having an energy of  $8.532 \pm 0.008$  MeV as the ground-state transition for capture by  $\text{Ni}^{60}$ .

TABLE II. Energies of ground-state gamma rays following the positron decay of  $\text{Cu}^{61}$ .

Energy (MeV)	Based on
$0.070 \pm 0.002$	0.082 $\text{Ba}^{133}$
$0.282 \pm 0.003$	0.316 $\text{Ir}^{192}$
$0.659 \pm 0.003$	0.662 $\text{Cs}^{137}$
$1.192 \pm 0.005$	1.173 $\text{Co}^{60}$

If however, one uses the  $\text{Cu}^{61}$  beta end point<sup>1,24</sup> and our  $\text{Ni}^{60}(p,\gamma)\text{Cu}^{61}$   $Q$  value,<sup>18</sup> the  $\text{Ni}^{60}(n,\gamma)\text{Ni}^{61}$   $Q$  value is calculated to be  $7.83 \pm 0.03$  Mev, which places the ground-state gamma transition within 3 kev of gamma ray  $D$ , which is well within the stated uncertainties of the experiments involved. Since the even-even nucleus  $\text{Ni}^{60}$  has even parity and zero spin, and since compound states formed by the addition of thermal neutrons would be  $\frac{1}{2}^+$ , a transition to the  $\frac{3}{2}^-$  ground state of  $\text{Ni}^{61}$  would be of the  $E1$  type and therefore quite probable. Therefore, gamma ray  $D$  is assigned as the  $\text{Ni}^{60}(n,\gamma)\text{Ni}^{61}$  ground-state transition.

It is almost certain that the proton group which Hoesterey attributed to the ground-state transition from the  $\text{Ni}^{60}(d,p)\text{Ni}^{61}$  reaction was actually the group from the  $\text{Ni}^{58}(d,p)\text{Ni}^{59}$  reaction leaving  $\text{Ni}^{59}$ , in the 875-kev state, even though he was using enriched isotopes. This argument is enhanced by the fact that Pratt,<sup>13</sup> using the same reaction, did not see the "ground-state" group of protons reported by Hoesterey, but did see the "first excited state" group which we believe was actually the ground-state transition.

After the present experiment was finished, Quisenberry *et al.*<sup>27</sup> published a new table of mass-spectrometer mass values. Their data are in considerable disagreement with the older work, but are in good agreement with the present experiment. Using their new mass values, they calculated that the ground-state gamma ray for the  $\text{Ni}^{60}(n,\gamma)\text{Ni}^{61}$  reaction should be  $44 \pm 11$  kev less than the energy of gamma ray  $D$ , and came to the tentative conclusion that gamma ray  $D$  did represent the  $\text{Ni}^{60}(n,\gamma)\text{Ni}^{61}$   $Q$  value. We concur in this conclusion and consider the 44-kev discrepancy to be not large enough to be concerned about.

The  $Q$  value for the inverse reaction  $\text{Ni}^{61}(\gamma,n)\text{Ni}^{60}$ , measured by means of threshold techniques by Sher *et al.*,<sup>2</sup> was previously discounted by Kinsey and Bartholomew because of uncertain isotopic assignment by Sher *et al.*, and because of disagreement with the above data of Hoesterey and Collins *et al.* Sher's result of  $-7.5 \pm 0.3$  Mev for the  $(\gamma,n)$   $Q$  value is, however, in satisfactory agreement with our results.

Figure 5 shows a collection of most of the relevant data concerning the energy levels of  $\text{Ni}^{59}$  and  $\text{Ni}^{61}$ . The columns from left to right present the data of references 13, 20, present, present, and 10, respectively. Where stated uncertainties are greater than  $\pm 10$  kev, they are shown by error bars on the energy level lines. The energy scale on the right is a measure of the high-energy gamma rays measured by Kinsey and Bartholomew for thermal-neutron capture by natural nickel. The letters were assigned by them to each gamma ray observed, and therefore do not necessarily represent energy levels in any particular nucleus. The numbers above each "gamma-ray line" represent the level energy assuming neutron capture by  $\text{Ni}^{58}$ , based on gamma ray  $A$  as the

ground-state transition. The numbers below the lines represent the level energy assuming neutron capture by  $\text{Ni}^{60}$ , based on gamma ray  $D$  as the ground-state transition.

The correlation of data from the  $\text{Co}^{59}(p,n)\text{Ni}^{59}$  and  $\text{Ni}^{58}(d,p)\text{Ni}^{59}$  reactions with the data from the  $\text{Ni}(n,\gamma)\text{Ni}$  reactions has been discussed in a previous communication.<sup>20</sup> The energy level assignments resulting from the positron decay of  $\text{Cu}^{59}$  and  $\text{Cu}^{61}$  are shown in the two columns beside the neutron-capture gamma lines. These assignments are based on coincidence studies described in Sec. II. The ground state of  $\text{Ni}^{61}$  has been drawn to match the position of gamma ray  $D$ , and that for  $\text{Ni}^{59}$  drawn to match gamma ray  $A$ .

A correspondence can be seen between the 0.463-Mev gamma ray, following the positron decay of  $\text{Cu}^{59}$ , and gamma ray  $B$ , previously assigned as the ground-state transition for  $\text{Ni}^{61}$ . The same statement holds for the 0.872-Mev gamma ray and gamma ray  $C$ . The 0.282-Mev gamma ray, following the decay of  $\text{Cu}^{61}$ , likewise corresponds to gamma ray  $E$ .

Since our assignments of the gamma rays following the positron decay of  $\text{Cu}^{61}$  to levels in  $\text{Ni}^{61}$  differ from the assignments of Owen, Cook, and Owen,<sup>1</sup> who assigned levels at 0.65, 0.93, and 1.00 Mev, it is worthwhile to compare our assignments with some recent data of Fagg *et al.*,<sup>28</sup> who studied the gamma rays following Coulomb excitation of  $\text{Ni}^{61}$  by 4-Mev alpha particles. They found gamma rays of 70, 282, and 657 kev. Their data indicate that these gamma rays correspond to states of the same values in agreement with our results and those of Nussbaum *et al.*<sup>26</sup>

We did not measure the positron end points directly, but using the  $\text{Ni}^{58}(n,\gamma)\text{Ni}^{59}$   $Q$  value<sup>10</sup> and our  $\text{Ni}^{58}(p,\gamma)\text{Cu}^{59}$   $Q$  value<sup>19</sup> we calculated the end point for the  $\text{Cu}^{59}$  decay to the  $\text{Ni}^{59}$  ground state to be  $3.76 \pm 0.03$  Mev. This is in good agreement with the expected end point predicted from beta-decay systematics by Nussbaum *et al.*,<sup>14</sup> and two direct measurements of  $3.4 \pm 0.5$  Mev from a Feather analysis by Lindner *et al.*<sup>15</sup> of the  $\beta$  absorption in aluminum, and  $3.74 \pm 0.1$  Mev from a magnetic  $\beta$ -spectrometer measurement by Prosser *et al.*<sup>22</sup>

However, according to a direct measurement by Yuasa *et al.*<sup>16</sup> (magnetic spectrometer), the end point is  $1.85 \pm 0.05$  Mev. Furthermore, their Kurie plot is straight, from the cutoff point to 0.5 Mev, indicating no transitions to excited states below 1.35 Mev. Since we observed gamma rays of 0.343, 0.463, 0.872, and 1.305 Mev in coincidence with positrons, we can conclude only that Yuasa *et al.* were not observing the decay of  $\text{Cu}^{59}$ .

It is of interest to attempt to correlate the results of two recent experiments concerning the low-energy gamma rays following thermal-neutron capture by natural nickel. These low-energy gamma rays have been

<sup>27</sup> Quisenberry, Scolman, and Nier, Phys. Rev. **104**, 461 (1956).

<sup>28</sup> Fagg, Geer, and Wolicki, Phys. Rev. **104**, 1073 (1956).

examined by Braid<sup>29</sup> at Chalk River and by Adyasevich *et al.*<sup>30</sup> of the U.S.S.R. Academy of Sciences. (The latter group also observed the high-energy gamma rays and were in good agreement with Kinsey and Bartholomew.) Both groups used the Compton recoil electrons, but Braid used a NaI crystal spectrometer, and Adyasevich *et al.* used a magnetic spectrometer. The results of the two essentially identical experiments are not in good agreement since the gamma rays which were observed by one group were not seen by the other and vice versa. However, with the energy level assignments discussed above, and by an examination of the published data curves of the two experiments, one can, by exercising a certain amount of judicious discrimination, give a reasonable explanation of both sets of data. Since the experiments were approximately concurrent, in neither of the published papers was the other reviewed or compared.

Because of the previous confusion concerning the energy levels of  $\text{Ni}^{59}$  and  $\text{Ni}^{61}$ , the above authors attempted to assign only a few of the low-energy gamma rays to isotopes, and some of these are given different assignments herein. The two sets of gamma rays are reproduced in Table III together with their respective relative intensities. The individual gamma rays will be discussed from the lowest energy up beginning with those of Adyasevich *et al.* The  $0.280 \pm 0.015$  Mev gamma ray is assigned to  $\text{Ni}^{61}$ , a ground-state transition from the 0.282-Mev state. In Fig. 5, it is a transition from *E* to *D*. Kinsey and Bartholomew measured the intensity of *E* to be 4%, and Adyasevich *et al.* report the 0.280-Mev gamma ray to be  $\geq 3.5\%$ . Braid's equipment has a low-energy cutoff in the neighborhood of 0.3 Mev, so it is not surprising that he did not observe the 0.280-Mev gamma ray.

The  $0.330 \pm 0.015$  Mev gamma ray could be a ground-state transition from the 0.342-Mev state of  $\text{Ni}^{59}$ , but this state is not fed by primary gamma rays, and it is not clear which gamma rays could be feeding it in a cascade. The problem here is one of intensity. The 0.330 Mev gamma ray was the most intense low-energy gamma ray ( $\geq 7\%$ ) observed by Adyasevich *et al.* So one would expect to observe the gamma rays feeding it. But none of the listed gamma rays fits neatly into such a scheme.

The  $0.436 \pm 0.015$  Mev gamma ray ( $\geq 3\%$ ) probably represents a transition from the 0.439-Mev state of  $\text{Ni}^{59}$ , but again it is not clear how the state is fed.

The  $0.467 \pm 0.008$  Mev gamma ray ( $\geq 6\%$ ) is a transition (*B-A* in Fig. 5) from the 0.465-Mev state of  $\text{Ni}^{59}$  and is fed by gamma ray *B* (14%). Our intensity problems would be solved if the 0.465-Mev state cascaded through the 0.439- and 0.342-Mev states about half the time. Such a possibility is extremely

TABLE III. The low-energy gamma rays following thermal-neutron capture by natural nickel, as reported by the following authors.

Peak number	Adyasevich <i>et al.</i>		Braid	
	Energy (Mev)	Intensity (photons per 100 neutron captures)	Energy (Mev)	Intensity (photons per 100 neutron captures)
28	$0.280 \pm 0.015$	$\geq 3.5$	$0.45 \pm 0.03$	8
27	$0.330 \pm 0.015$	$\geq 7$	$0.86 \pm 0.03$	3
26	$0.436 \pm 0.015$	$\geq 3$	$1.24 \pm 0.03$	2
25	$0.467 \pm 0.008$	$\geq 6$	$2.06 \pm 0.03$	3
24	$(1.10 \pm 0.03)$	$\geq 2$	$2.68 \pm 0.03$	2
23	$(1.53 \pm 0.03)$	$\geq 1$		
22	$(1.74 \pm 0.03)$	$\geq 1$		
21	$(2.15 \pm 0.03)$	$\geq 2$		
20	$(3.03 \pm 0.04)$	$\geq 1$		
19	$(3.17 \pm 0.06)$	$\geq 1$		
18	$(3.67 \pm 0.03)$	$\geq 1$		

unlikely, however, because in the  $\beta^+$  decay of  $\text{Cu}^{59}$ , the 0.465-Mev level was excited, but no cascades from it were observed.

Braid's  $0.45 \pm 0.03$  Mev gamma ray (8%) is probably the unresolved combination of the above two gammas.

The  $1.10 \pm 0.03$  Mev gamma ray ( $\geq 2\%$ ) could be a cascade between the 1.964-Mev state and the 0.875-Mev state (*G-C*). However, that seems unlikely for intensity reasons. The 1.964-Mev state is fed by gamma ray *G* (0.5%), and by no other apparent means, and possibly exhibits a ground-state transition accounting for  $\sim 1\%$  of the gamma rays (discussed below). Another possibility is that gamma ray *N* comes from  $\text{Ni}^{63}$  and represents a state at  $1.14 \pm 0.02$  Mev in  $\text{Ni}^{63}$ . (For reasons discussed below, gamma ray *H* is assigned as the ground-state transition in  $\text{Ni}^{63}$ .) The resulting ground-state transition (*N-H*) then could be the  $1.10 \pm 0.03$  Mev gamma ray.

The  $1.53 \pm 0.03$  Mev gamma ray ( $\geq 1\%$ ) could be a cascade between the 1.964- and 0.439-Mev states. But again intensity considerations make it unlikely. Another possibility is as follows. If *L* comes from  $\text{Ni}^{61}$ , a cascade from the 1.83-Mev state of  $\text{Ni}^{61}$  thus formed, to the 0.282-Mev state (*L-E*) would be  $1.55 \pm 0.02$  Mev. In Fig. 5, the number under the line for gamma ray *L* refers to gamma ray *K*.

The  $1.74 \pm 0.03$  Mev gamma ray ( $\geq 1\%$ ) could be a cascade from the 2.16-Mev state of  $\text{Ni}^{59}$  to the 0.439-Mev state. Two other possibilities are a transition from the 1.70-Mev state to the ground state (unlikely because the 1.70-Mev state is apparently not excited here) or the 1.79-Mev state to the ground state.

The  $3.03 \pm 0.04$  Mev gamma ray ( $\geq 1\%$ ) could be a transition (*L-A*) from the  $3.01 \pm 0.02$ -Mev state of  $\text{Ni}^{59}$ , if gamma ray *L* (0.3%) comes from  $\text{Ni}^{59}$ .

The  $3.17 \pm 0.06$  Mev gamma ray ( $\geq 1\%$ ) is probably a ground-state transition (*M-A*) from the  $3.19 \pm 0.02$  Mev state of  $\text{Ni}^{59}$  fed by gamma ray *M* (3%).

Braid's  $0.86 \pm 0.03$  Mev gamma ray (3%) has only a very weak, if any, counterpart in Adyasevich's curve.

<sup>29</sup> T. H. Braid, Phys. Rev. **102**, 1109 (1956).

<sup>30</sup> Adyasevich, Groshev, Demidov, and Lutsenko, Atomnaya Energiya **1**, 28 (1956). An English translation by L. C. Ronson is available [J. Nuclear Energy **II**, **3**, 325 (1956)].

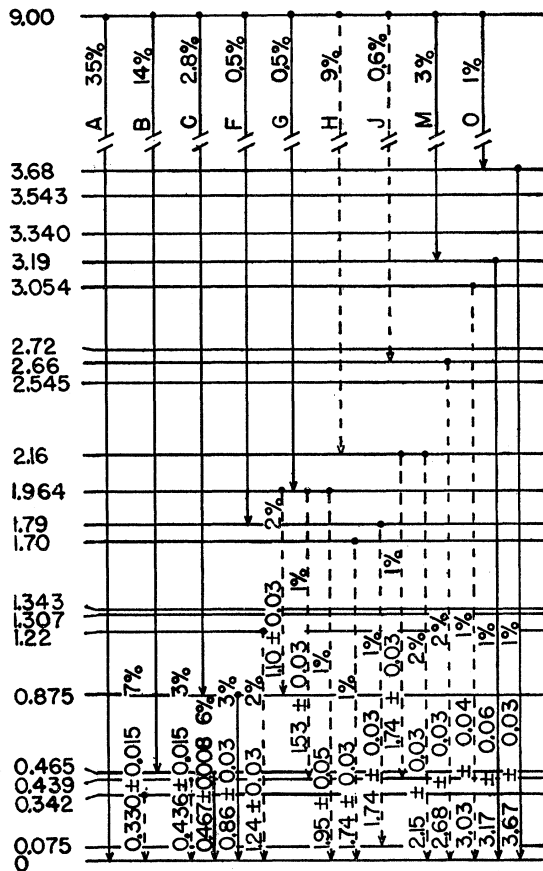


FIG. 8. A summary of the possible low-energy thermal-neutron-capture gamma rays of Adyasevich *et al.*, and of Braid, with respect to energy levels of  $\text{Ni}^{59}$  known from other experiments. The letters and relative intensities on the high-energy gamma transitions are those of Kinsey and Bartholomew.

This gamma ray corresponds to the 0.875-Mev state of  $\text{Ni}^{59}$ , a transition from *C* (2.8%) to *A* in Fig. 5.

The  $1.24 \pm 0.03$  Mev gamma ray (2%) of Braid is apparently evident in the published curve of Adyasevich *et al.* between their peaks 23 and 24. This gamma ray could be either a ground-state transition from the 1.22-Mev state of  $\text{Ni}^{59}$  (not fed by primary gammas) or the 1.24-Mev state of  $\text{Ni}^{61}$  if gamma ray *I* (2%) feeds such a state.

Braid's  $2.06 \pm 0.03$  Mev gamma ray (3%) could be the same as the 2.06-Mev gamma ray of Prosser *et al.*,<sup>22</sup> following the positron decay of  $\text{Cu}^{69}$ . However, since their gamma ray was very weak and was not observed in the present experiment, and since Braid's gamma ray could be a doublet, judging from his published curve, this assignment seems improbable. The spectrum of Adyasevich *et al.* also gives evidence for such a doublet, with one peak at  $2.15 \pm 0.03$  Mev (their peak 21) and another about 1.95 Mev. These could be the ground-state transitions from the states at 1.964 and 2.15 Mev in  $\text{Ni}^{59}$ , fed by gamma rays *G* and *H*, respectively.

The  $2.68 \pm 0.03$  Mev gamma ray (2%) of Braid corresponds to a peak in the spectrum of Adyasevich *et al.* between their numbers 20 and 21. Such a peak was drawn but not numbered. If the gamma ray is real, it probably corresponds to a transition from the 2.66-Mev state of  $\text{Ni}^{59}$ , if gamma ray *J* (0.6%) feeds such a state.

A summary of the possible assignments for  $\text{Ni}^{59}$  discussed above is given in Fig. 8. The reasonably certain assignments are shown by solid arrows. The less certain assignments are indicated by broken arrows. The letters on the high-energy transitions are the same as Fig. 5.

From intensity considerations, it appears very unlikely that gamma ray *H* comes entirely from  $\text{Ni}^{59}$ . Gamma ray *H* corresponds in energy to the 2.15-Mev level from the  $\text{Co}^{59}(p,n)\text{Ni}^{59}$  reaction, and from reference 30 there is some evidence of a low-energy transition from such a state. Thus, it is reasonable that gamma ray *H* is an unresolved combination of two gamma rays with practically the same energy. Of the 9% relative intensity of *H*, if only 3% or less can be attributed to  $\text{Ni}^{59}$ , the other 6% must come from  $\text{Ni}^{61}$  or  $\text{Ni}^{63}$ . But there is no known state in  $\text{Ni}^{61}$  corresponding to *H*. Furthermore, since the total contributions expected<sup>31</sup> from each product nuclide  $\text{Ni}^{59}$ ,  $\text{Ni}^{61}$ , and  $\text{Ni}^{63}$  are 71%, 15%, and 13%, respectively, and since *D* and *E*, with a combined intensity of 10.5%, are already attributed to  $\text{Ni}^{61}$ , it appears quite likely that most, if not all, of *H* comes from  $\text{Ni}^{63}$ , even though from mass-spectrometer measurements<sup>7</sup> and the decay of  $\text{Ni}^{63}$ , the  $\text{Ni}^{62}(n,\gamma)\text{Ni}^{63}$  ground-state transition should be  $6.0 \pm 0.1$  Mev. Gamma ray *H* is  $6.839 \pm 0.010$  Mev.

TABLE IV. Summary of energy levels in  $\text{Ni}^{59}$  and  $\text{Ni}^{61}$ .<sup>a</sup>

$\text{Ni}^{59}$ energy (Mev)	Excited by	$\text{Ni}^{61}$ energy (Mev)	Excited by
0	b, c, d, e	0	f, g, h
$0.342 \pm 0.004$	(b), (c), d, e	$0.070 \pm 0.002$	h, i
$0.439 \pm 0.005$	(b), e	$0.282 \pm 0.003$	f, h, i
$0.465 \pm 0.010$	b, (c), d	$0.659 \pm 0.003$	h, i
$0.875 \pm 0.005$	b, c, d	$1.192 \pm 0.005$	h
$1.22 \pm 0.01$	c, e		
$1.305 \pm 0.005$	d		
$1.343 \pm 0.010$	e		
$1.70 \pm 0.01$	c, d		
$1.79 \pm 0.01$	b, e		
$1.964 \pm 0.010$	b, e		
$(2.15 \pm 0.01)$	(b), (e)		
$2.545 \pm 0.010$	e		
$(2.72 \pm 0.01)$	(e)		
$3.054 \pm 0.010$	e		
$3.19 \pm 0.02$	b, e		

<sup>a</sup> Energies and references in parentheses refer to uncertain assignments.

<sup>b</sup>  $\text{Ni}^{58}(n,\gamma)\text{Ni}^{59}$  (thermal neutrons, reference 10).

<sup>c</sup>  $\text{Ni}^{58}(d,p)\text{Ni}^{59}$  (3-Mev d, reference 13).

<sup>d</sup>  $\text{Cu}^{69}(\beta^+)\text{Ni}^{59}$  (present work).

<sup>e</sup>  $\text{Co}^{59}(p,n)\text{Ni}^{59}$  (neutron thresholds, reference 20).

<sup>f</sup>  $\text{Ni}^{59}(n,\gamma)\text{Ni}^{60}$  (thermal neutrons, reference 10).

<sup>g</sup>  $\text{Ni}^{60}(d,p)\text{Ni}^{61}$  (3-Mev d, reference 13).

<sup>h</sup>  $\text{Cu}^{61}(\beta^+)\text{Ni}^{61}$  (present work).

<sup>i</sup>  $\text{Ni}^{61}(\alpha,\alpha^+)\text{Ni}^{61}$  (Coulomb excitation, reference 28).

<sup>31</sup> *Nuclear Level Schemes, A=40—A=92*, compiled by Way, King, McGinnis, and van Lieshout, U. S. Atomic Energy Commission Report TID-5300 (U. S. Government Printing Office, Washington, D. C., 1955).



To test this hypothesis, the  $\text{Ni}^{62}(n,\gamma)\text{Ni}^{63}$   $Q$  value was determined from the  $\text{Ni}^{62}(p,\gamma)\text{Cu}^{63}$   $Q$  value ( $6.13 \pm 0.03$  Mev) measured in this laboratory together with the  $\text{Ni}^{62}(\beta^-)\text{Cu}^{63}$   $Q$  value<sup>32</sup> of  $0.063 \pm 0.002$  Mev. The  $\text{Ni}^{62}(n,\gamma)\text{Ni}^{63}$  ground-state transition is thus calculated to be  $6.85 \pm 0.03$  Mev which may be compared with Kinsey and Bartholomew's measurement of  $6.839 \pm 0.010$  Mev for gamma ray  $H$ . It is therefore reasonably certain that gamma ray  $H$  (at least in part) comes from neutron capture by  $\text{Ni}^{62}$ . The latest mass-spectrometer measurements<sup>27</sup> are in agreement with this conclusion, since the  $\text{Ni}^{62}(n,\gamma)\text{Ni}^{63}$  ground-state transition calculated from them is  $6.825 \pm 0.010$  Mev, and Quisenberry *et al.* independently arrived at the same assignment of  $H$ .

The combined intensities of gamma rays  $A$ ,  $B$ ,  $C$ ,  $F$ ,  $G$ , and  $M$ , assigned to the  $\text{Ni}^{59}$  product nuclide, are 56%. Gamma rays  $D$  and  $E$ , assigned to the  $\text{Ni}^{61}$  product nuclide, have a combined intensity of 10.5%. Gamma ray  $H$ , assigned primarily to  $\text{Ni}^{63}$ , has an intensity of 9%. These combined intensities may be compared with the expected relative intensities<sup>31</sup> of these isotopes of 71%, 15%, and 13%, respectively.

Table IV gives a compilation of the energy levels in both  $\text{Ni}^{59}$  and  $\text{Ni}^{61}$ , and the reaction in which each level is observed. Nussbaum *et al.*<sup>26</sup> observed that the energy levels in  $\text{Ni}^{61}$  are given within about 5% accuracy by the formula  $E = 73n^2$  (kev) where  $n$  is the number of the excited state. Similar formulas have been observed for neighboring nuclides. But it is not apparent that such a formula holds for  $\text{Ni}^{59}$ , because no excited state has been observed below 343 kev.

The similarity of level structure in  $\text{Ni}^{59}$ ,  $\text{Ni}^{61}$ ,  $\text{Cu}^{59}$ , and  $\text{Cu}^{61}$  is rather striking. (For information on levels in the two copper isotopes, see reference 19.) Table V gives the gamma rays from the Cu isotopes following proton capture by  $\text{Ni}^{58}$  and  $\text{Ni}^{60}$ , and from the Ni isotopes following positron decay of the Cu isotopes.

$\text{Ni}^{59}$  and  $\text{Cu}^{59}$  are somewhat analogous to  $\text{O}^{19}$  and  $\text{F}^{19}$  since  $\text{Ni}^{59}$  has three neutrons outside a doubly closed shell ( $Z=N=28$ ) and  $\text{Cu}^{59}$  has 2 neutrons and 1 proton outside the same shell. On this analogy, one would not

TABLE V. Gamma rays from four nuclides showing similarities in their spectra. The  $\text{Cu}^{59}$  and  $\text{Cu}^{61}$  gamma rays arise from proton capture by  $\text{Ni}^{58}$  and  $\text{Ni}^{60}$ . The  $\text{Ni}^{59}$  and  $\text{Ni}^{61}$  gamma rays follow the positron decay of the Cu isotopes.

$\text{Ni}^{59}$	$\text{Cu}^{59}$	$\text{Ni}^{61}$	$\text{Cu}^{61}$
		0.070	(0.08)
0.343		0.282	
0.463	0.492		0.468
0.872	0.908	0.659	0.96
1.305	1.38	1.192	1.30, 1.38
1.70	1.78		1.63
(2.06)	2.00		1.91

expect the low levels to be similar because the  $T_z$  component of isotopic spin for  $\text{Cu}^{59}$  is  $\frac{1}{2}$ , whereas it is  $\frac{3}{2}$  for  $\text{Ni}^{59}$ . Normally, nuclides with higher  $T_z$  have considerably fewer levels and their analogs in the lower  $T_z$  nucleus are rather high in energy.

Using the elementary concepts of isotopic spin multiplets, one can calculate where the first  $T = \frac{3}{2}$  state should lie in  $\text{Cu}^{59}$ . The Coulomb effect on the net binding energy can be determined from the beta-decay energies of mirror nuclei. If a plot is made of the decay energies of mirror nuclei as far as they have been observed (up to and including  $Z=21$ ) and the curve is extrapolated to  $Z=29$  (Cu), a value of about 6.5 Mev is obtained for the hypothetical decay of  $\text{Cu}^{57}$  to  $\text{Ni}^{57}$ . Combining this with the positron decay  $Q$  value<sup>22</sup> of  $\text{Cu}^{59}$ , one concludes that the specifically nuclear forces require the binding energy of  $\text{Cu}^{59}$  to be about 2.7 Mev greater than that of  $\text{Ni}^{59}$ . Thus, one would expect on this basis a  $T = \frac{3}{2}$  state at about 2.7 Mev in  $\text{Cu}^{59}$  corresponding to the ground state of  $\text{Ni}^{59}$ . The region in  $\text{Cu}^{59}$  between 2.4 and 4.3 Mev is completely unexplored.<sup>19</sup>

These simple concepts, therefore, do not explain the similarity of gamma-ray spectra obtained from the two nuclides. The information in Table V is more suggestive of mirror nuclei than of a  $T_z = \frac{1}{2}$ ,  $T_z = \frac{3}{2}$  pair. This similarity can hardly be discounted as purely accidental. A theoretical investigation might yield some interesting results.

<sup>32</sup> R. W. King, *Revs. Modern Phys.* **26**, 327 (1954).